



Simplest Monodentate Imidazole Stabilization of the oxy-Tyrosinase Cu₂O₂ Core: Phenolate Hydroxylation through a Cu^{III} Intermediate

Linus Chiang, William Keown, Cooper Citek, Erik C. Wasinger, and T. Daniel P. Stack*

Abstract: Tyrosinases are ubiquitous binuclear copper enzymes that oxygenate to Cu^{II}₂O₂ cores bonded by three histidine N τ -imidazoles per Cu center. Synthetic monodentate imidazole-bonded Cu^{II}₂O₂ species self-assemble in a near quantitative manner at –125°C, but N π -ligation has been required. Herein, we disclose the syntheses and reactivity of three N τ -imidazole bonded Cu^{II}₂O₂ species at solution temperatures of –145°C, which was achieved using a eutectic mixture of THF and 2-MeTHF. The addition of anionic phenolates affords a Cu^{III}₂O₂ species, where the bonded phenolates hydroxylate to catecholates in high yields. Similar Cu^{III}₂O₂ intermediates are not observed using N π -bonded Cu^{II}₂O₂ species, hinting that N τ -imidazole ligation, conserved in all characterized Ty, has functional advantage beyond active-site flexibility. Substrate accessibility to the oxygenated Cu₂O₂ core and stabilization of a high oxidation state of the copper centers are suggested from these minimalistic models.

Tyrosinases (Ty) are ubiquitous binuclear Cu enzymes responsible for melanin biosynthesis through regioselective tyrosine aromatic hydroxylation to form catechols, and their subsequent oxidation to quinones. Spectroscopic and X-ray crystallographic analysis of the oxygenated form of tyrosinase (oxyTy) reveals a side-on μ - η^2 : η^2 peroxide dicopper (II) (^SP) species ligated exclusively by six histidine residues through the τ -nitrogen (N τ) of each imidazole (Figure 1).^[1] This results in a highly accessible ^SP Cu₂O₂ core where the 4-substituents of the imidazoles are positioned remotely. This N τ -ligated ^SP core is conserved in oxygenated hemocyanin (oxyHc) proteins,^[2] an evolutionary descendant of Ty^[3] responsible for reversible dioxygen (O₂) uptake and storage.^[1b,4] The reactivity difference between oxyTy and oxyHc is attributed to substrate access to the oxygenated Cu₂O₂ core,^[5] as partially denatured hemocyanin proteins can exhibit mono-oxygenase reactivity.^[6] Alternatively, more sterically demanding and less-flexible π -nitrogen (N π) imidazole ligation is observed exclusively in electron-transfer blue-copper sites, suggesting N τ -ligation may serve a functional purpose, such as

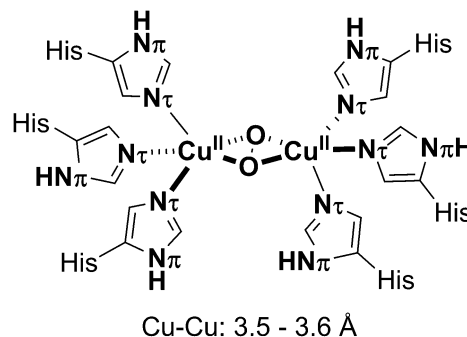


Figure 1. The conserved ligation structure of oxyTy.^[1]

providing flexibility for O₂ capture, allowing substrate access to the oxygenated ^SP core, and potentially stabilizing higher oxidation states of copper in the mono-oxygenase reaction.^[1c,7]

Synthetic ^SP analogues of oxyTy have received extensive attention over the last few decades.^[4a,8] Stoichiometric phenolate oxidation to catecholates is possible at the low reaction temperatures required to stabilize most synthetic ^SP species, although several catalytic systems operating at elevated temperatures are now known.^[9] These complexes are generally supported by multi-nucleating alkyl amines or heterocycles, such as pyridines, pyrazoles, or benzimidazoles. However, synthetic ^SP species exclusively ligated by imidazoles, especially by imidazoles bearing an N–H group,^[10] are limited.^[8b,c,11] Over 30 years ago, Zuberbühler reported that Cu^I bonded by monodentate imidazoles can react with O₂ under ambient aqueous conditions via a binuclear intermediate, as inferred from kinetic measurements.^[12] In the early 1990s, Zuberbühler and Karlin subsequently investigated the oxygenation of [Cu^I(1,2-dimethylimidazole)₃]⁺ at lower temperatures using weakly coordinating anions in aprotic solvents,^[13] but the nature of those intermediates could not be assigned definitively.

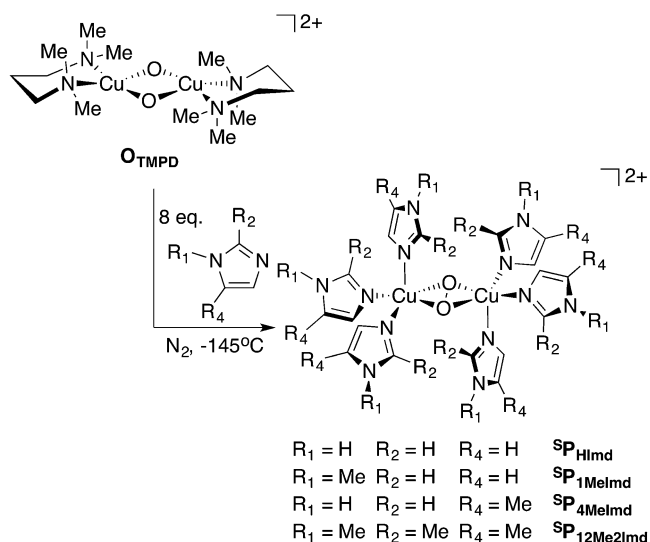
More recently, the near quantitative self-assembly of a series of imidazole-ligated ^SP species (^SP_{RImd}) by direct oxygenation of [Cu^I(RImd)₃]⁺ at –125°C in 2-methyltetrahydrofuran (2-MeTHF) was disclosed.^[10] At these temperatures, deleterious reactions along the oxygenation and subsequent ^SP_{RImd} formation pathways are presumably eliminated as yields greater than 90% are realized. However, N π -ligation with 2- or 4,5-substituted imidazoles (e.g., 1,2-dimethylimidazole or 4,5-dimethylimidazole) was necessary for good formation yields; no significant formation of ^SP_{RImd} species with N τ -ligation (e.g., 1-methylimidazole) was observed. Herein, we present the synthesis and characterization of the first examples of ^SP_{RImd} species bearing N τ

[*] Dr. L. Chiang, W. Keown, Dr. C. Citek, Prof. T. D. P. Stack
Department of Chemistry, Stanford University
Stanford, CA 94305 (USA)
E-mail: stack@stanford.edu
Dr. E. C. Wasinger
Department Chemistry and Biochemistry
California State University
Chico, CA 95929 (USA)

Supporting information for this article, including experimental, instrumentation, and computational details, can be found under: <http://dx.doi.org/10.1002/anie.201605159>.

ligation by the simplest imidazoles (1-methyl, 4-methyl, and unsubstituted imidazole), and their reactivity with phenolates to form a transient but detectable Cu^{III} intermediate at -145°C that subsequently yield their corresponding hydroxylated products.

While direct oxygenation of $[\text{Cu}^{\text{I}}(\text{RImd})_3]^+$ to $^{\text{S}}\text{P}_{\text{RImd}}$ species with these simplest imidazoles at -145°C is possible, the yields are improved significantly using an indirect ligand exchange pathway, designated as core-capture (Scheme 1).^[14]



Scheme 1. Core-capture synthetic methodology to generate $^{\text{S}}\text{P}_{\text{RImd}}$ species.

The bis- μ -oxide dicopper (III) species of tetramethylpropylenediamine (O_{TMPD}) is a robust $\text{Cu}-\text{O}_2$ compound that forms fully at -80°C .^[15] At -125°C , the addition of 8 equiv of 1,2-dimethylimidazole to O_{TMPD} yields an identical spectrum to that achieved by direction oxygenation of $[\text{Cu}^{\text{I}}(1,2\text{-dimethylimidazole})_3]^+$ (Supporting Information, Figure S1); neither spectra appreciably changed over 30 minutes. By contrast, adding 8 equiv of one of the simplest imidazoles to O_{TMPD} at -125°C only leads to transient formation of the target $^{\text{S}}\text{P}_{\text{RImd}}$ species. To slow thermal decay, lower solution temperatures are necessary. With the freezing point of 2-MeTHF at -136°C , only viscous, unworkable slurries were possible below -125°C in our experimental setup. A eutectic mixture of 2-MeTHF:THF (4:1), cooled externally by a slurry of pentane:2-methylbutane (4:3) with liquid N_2 , yields stable solution temperatures of -145°C while maintaining millimolar concentrations of charged copper complexes. Adding 8 equiv of each of the simplest imidazoles to O_{TMPD} at -145°C leads to full formation of their respective $\text{N}\tau$ -ligated $^{\text{S}}\text{P}_{\text{RImd}}$ species in approximately 5 minutes (Figure 2). While $^{\text{S}}\text{P}_{1\text{MeImd}}$ is stable indefinitely at -145°C , $^{\text{S}}\text{P}_{4\text{MeImd}}$ and $^{\text{S}}\text{P}_{\text{HImd}}$, containing $\text{N}-\text{H}$ imidazoles, decay with half-lives ($t_{1/2}$) of 30 and 15 minutes, respectively.

The yield of $^{\text{S}}\text{P}_{1\text{MeImd}}$ is greater than 95 %, assessed through a subsequent core-capture experiment using tris[(2-dimethylamino)ethyl]amine (Me_6Tren) to yield an end-on $\text{trans}-\mu-\eta^1:\eta^1$ peroxide dicopper (II) ($^{\text{T}}\text{P}_{\text{Me6Tren}}$) complex (Figure S4).^[10] The

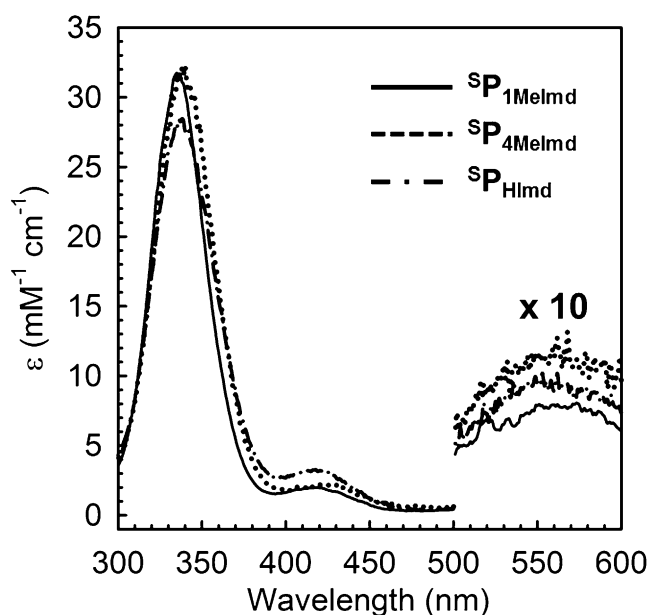


Figure 2. UV/Vis absorption spectra of $^{\text{S}}\text{P}_{1\text{MeImd}}$ (solid, $\lambda_{\text{max}} = 335, 417, 560 \text{ nm}$), $^{\text{S}}\text{P}_{4\text{MeImd}}$ (dotted, $\lambda_{\text{max}} = 338, 423, 560 \text{ nm}$), and $^{\text{S}}\text{P}_{\text{HImd}}$ (dash-dotted, $\lambda_{\text{max}} = 337, 417, 550 \text{ nm}$) generated from O_{TMPD} at -145°C . $[\text{Cu}] = 0.9 \text{ mM}$, 0.1 cm path , 4:1 2-MeTHF/THF, -145°C .

comparable extinction coefficients (340 nm) of the ligand-to-metal charge transfer (LMCT) band for $^{\text{S}}\text{P}_{4\text{MeImd}}$ and $^{\text{S}}\text{P}_{\text{HImd}}$ suggests comparably good formation yields (Table 1).

Solution Cu K-edge X-ray absorption spectroscopy (XAS) of $^{\text{S}}\text{P}_{1\text{MeImd}}$, $^{\text{S}}\text{P}_{4\text{MeImd}}$, and $^{\text{S}}\text{P}_{\text{HImd}}$ exhibit pre-edge energies of near 8979 eV, which are characteristic of the Cu^{II} oxidation state (Figure S5).^[10,16] The extended X-ray absorption fine structure (EXAFS) analyses of $^{\text{S}}\text{P}_{1\text{MeImd}}$ and $^{\text{S}}\text{P}_{4\text{MeImd}}$ provide Cu–Cu distances in the 3.55–3.57 Å range, which are similar to other characterized $^{\text{S}}\text{P}_{\text{RImd}}$ species (Table 1, Figures S6–S7). EXAFS fitting of $^{\text{S}}\text{P}_{\text{HImd}}$ was complicated by its thermal instability.

Broken symmetry density functional theory (DFT) calculations at a B3LYP/6-31g(d)/SMD^{THF} level in C_i symmetry optimize $^{\text{S}}\text{P}_{1\text{MeImd}}$, $^{\text{S}}\text{P}_{4\text{MeImd}}$, and $^{\text{S}}\text{P}_{\text{HImd}}$ to planar $\text{Cu}^{\text{II}}_2\text{O}_2$ cores with Cu–Cu distances of approximately 3.63 Å, in reasonable agreement with their experimental EXAFS metrical parameters (Table 1).^[10] In addition, shorter Cu–ligand bond distances ($^{\text{S}}\text{P}_{1\text{MeImd}}$: Cu– $\text{N}_{\text{eq}} = 1.99 \text{ Å}$, Cu– $\text{N}_{\text{ax}} = 2.14 \text{ Å}$, Cu–O = 1.96 Å; $^{\text{S}}\text{P}_{12\text{Me2Imd}}$: Cu– $\text{N}_{\text{eq}} = 2.00 \text{ Å}$, Cu– $\text{N}_{\text{ax}} = 2.18 \text{ Å}$, Cu–O = 1.97 Å) and slight lengthening of the O–O bond is predicted ($^{\text{S}}\text{P}_{1\text{MeImd}}$: O–O = 1.48 Å; $^{\text{S}}\text{P}_{4\text{MeImd}}$: O–O = 1.47 Å; $^{\text{S}}\text{P}_{\text{HImd}}$: O–O = 1.48 Å; $^{\text{S}}\text{P}_{12\text{Me2Imd}}$: O–O = 1.47 Å). An elongated O–O bond is consistent with greater back-bonding from the Cu center into the peroxide σ^* orbital afforded by stronger bonds by the imidazole ligands.^[17]

The UV/Vis absorption spectra of $^{\text{S}}\text{P}_{1\text{MeImd}}$, $^{\text{S}}\text{P}_{4\text{MeImd}}$, and $^{\text{S}}\text{P}_{\text{HImd}}$ all exhibit an intense UV feature, along with two weak and broad visible features (Figure 2, Table 1).^[10] The LMCT UV feature^[18] is blue-shifted markedly from the 344 nm feature of $^{\text{S}}\text{P}_{12\text{Me2Imd}}$ and $^{\text{S}}\text{P}_{2\text{MeImd}}$, both bonded by $\text{N}\tau$ -ligating imidazoles (Table 1, Entries C and D). This is consistent with stronger imidazole bonding to the $\text{Cu}^{\text{II}}_2\text{O}_2$ core relative to other $^{\text{S}}\text{P}_{\text{RImd}}$ species.

Table 1: Physical properties of $^{\text{S}}\text{P}_{\text{RImd}}$ species formed by core-capture at -145°C .

Entry	Compound ^[a]	UV/Vis: λ_{max} , nm (ϵ , $\text{mM}^{-1}\text{cm}^{-1}$) ^[a,b]	Metrical parameters: EXAFS, \AA , ^[c] (DFT, \AA) ^[d]				
			Cu–Cu	Cu–N _{eq} /O	Cu–O	Cu–N _{ax}	O–O
A	$^{\text{S}}\text{P}_{1\text{MeImd}}$	335 (32.2), 417 (2.1), 560 (1.0)	3.55 (3.63)	1.95 (1.99)	(1.96)	2.24 (2.15)	(1.48)
B	$^{\text{S}}\text{P}_{4\text{MeImd}}$	338 (31.9), 423 (2.2), 560 (1.2)	3.57 (3.63)	1.96 (1.99)	(1.96)	2.20 (2.14)	(1.47)
C	$^{\text{S}}\text{P}_{12\text{Me2Imd}}^{\text{[b]}}$	344 (30.6), 428 (1.9), 560 (1.0)	3.57 (3.66)	1.95 (2.00)	(1.97)	2.21 (2.18)	(1.47)
D	$^{\text{S}}\text{P}_{2\text{MeImd}}^{\text{[b]}}$	344 (29.6), 425 (1.6), 560 (1.1)	3.58 (3.66)	1.96 (2.00)	(1.97)	2.23 (2.17)	(1.47)

[a] SbF_6^- , 4:1 2-MeTHF/THF. [b] See Ref. [10] for further characterization. [c] Resolution $\pm 0.01 \text{ \AA}$. [d] Optimized at B3LYP/6-31g(d)/SMD^{THF} level of theory in C_i symmetry.

Time-dependant DFT spectra of $^{\text{S}}\text{P}_{1\text{MeImd}}$, $^{\text{S}}\text{P}_{4\text{MeImd}}$, and $^{\text{S}}\text{P}_{\text{HImd}}$ are similar to their experimental spectra (Figure S8), as well as other $^{\text{S}}\text{P}_{\text{RImd}}$ species. Three significant transitions are predicted that are blue-shifted from other $^{\text{S}}\text{P}_{\text{RImd}}$ species. Natural Transition Orbital (NTO) analysis^[19] reveals that the most intense experimental absorbance at 335 nm is an in-plane peroxide $\pi_{\text{O}}^* \rightarrow d_{xy}$ transition, while the broad transition near 550 nm is an out-of-plane peroxide $\pi_{\text{v}}^* \rightarrow d_{xy}$, both consistent with previous assignments (Figure S9).^[18] The 417 nm feature, which was also observed and predicted for $^{\text{S}}\text{P}_{12\text{Me2Imd}}$ and $^{\text{S}}\text{P}_{2\text{MeImd}}$, is assigned as an imidazole $\pi^* \rightarrow d_{xy}$ from the NTO analyses (Figure S9).^[10]

The origin of blue-shifting for the $\pi_{\text{O}}^* \rightarrow d_{xy}$ transition of $^{\text{S}}\text{P}_{1\text{MeImd}}$ in comparison to $^{\text{S}}\text{P}_{12\text{Me2Imd}}$ was probed by TD-DFT. $^{\text{S}}\text{P}_{12\text{Me2Imd}}$ optimized in C_i symmetry exhibits a predicted transition at 349 nm. Removal of the 2-methyl substituent without further optimization results only in a 1 nm blue-shifted absorbance at 348 nm. Subsequent C_i symmetric optimization results in a slight contraction of coordinative bond distances ($\Delta\text{Cu–N}_{\text{avg}} = 0.02 \text{ \AA}$, $\Delta\text{Cu–Cu} = 0.03 \text{ \AA}$), affording $^{\text{S}}\text{P}_{1\text{MeImd}}$ with a 338 nm transition, a 10 nm blue-shift. This supports strongly that the observed blue-shifting is associated with stronger imidazole bonding to the metal center, corresponding from a reduction in ligand steric demands from $\text{N}\pi$ to $\text{N}\tau$ ligation. The increased experimental intensity of this LMCT feature for $^{\text{S}}\text{P}_{1\text{MeImd}}$ compared to $^{\text{S}}\text{P}_{12\text{Me2Imd}}$ further supports enhanced covalency in these contracted bonds.

While $^{\text{S}}\text{P}_{12\text{Me2Imd}}$ is favored thermodynamically over $^{\text{S}}\text{P}_{1\text{MeImd}}$ with respect to ligand substitution as established by ligand competition experiments (Figures S10 and S11), the increased steric demands of the ligating imidazoles consequently preclude substrate access to the $^{\text{S}}\text{P}$ core. Indeed, $^{\text{S}}\text{P}_{1\text{MeImd}}$ reacts rapidly and stoichiometrically with 0.5 equiv of 5,6-isopropylidene-L-ascorbic acid (H_2Asc), a net two-electron, two-proton reductive substrate, upon mixing at -145°C (Figure S12).^[20] $^{\text{S}}\text{P}_{12\text{Me2Imd}}$ exhibits essentially no reactivity towards H_2Asc under the same conditions, and only reacts in a pseudo-first-order manner in the presence of 20 equiv of H_2Asc ($t_{1/2} = 2 \text{ min}$) at -145°C (Figure S13). This highlights that $\text{Cu}^{\text{II}}_2\text{O}_2$ core exposure, by minimizing ligand steric demands, facilitates substrate access and rapid reaction with exogenous substrates.

The effects of increasing substrate access to the Cu_2O_2 core is further demonstrated through phenolate reactivity, in which $^{\text{S}}\text{P}_{1\text{MeImd}}$ reacts with 4 equiv of sodium 15-crown-5,2-*tert*-butyl-4-cyano phenolate at -145°C to form an intermediate

species in 1 minute (thermal decay $t_{1/2} = 10 \text{ min}$, Figure 3). Formation of a similar intermediate is not observed for $^{\text{S}}\text{P}_{12\text{Me2Imd}}$, although comparable yields of the catechol product are detected.

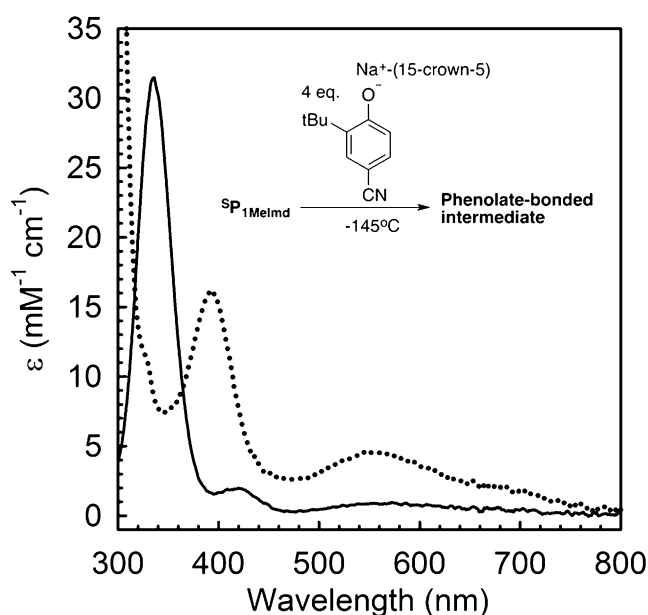


Figure 3. UV/Vis absorption spectra of a phenolate-bonded Cu^{III} intermediate (dotted, $\lambda_{\text{max}} = 394, 555, 650 \text{ nm}$) generated from $^{\text{S}}\text{P}_{1\text{MeImd}}$ (solid) at -145°C . $[\text{Cu}] = 0.9 \text{ mM}$, 0.1 cm path, 4:1 2-MeTHF/THF, -145°C .

Cu K-edge XAS analysis supports this intermediate as a bis- μ -oxide dicopper (III) species based on its pre-edge energy of 8980.2 eV and a characteristic 2.8 \AA Cu–Cu distance (Figures S14 and S15). While its identity is currently under investigation, this intermediate is ligated exclusively with imidazoles, phenolates, and O_2 -based ligands.^[21] A Cu^{III} -containing species coordinated by such biologically relevant ligands is unprecedented, and its characterization may provide insight into the active hydroxylating oxidant of tyrosinases.^[4a,22]

Demonstrated here is the formation and stabilization of three previously unobserved $^{\text{S}}\text{P}_{\text{RImd}}$ species supported by the simplest imidazoles at -145°C . These imidazoles contain no substituent adjacent to the ligating nitrogen atom, allowing for $\text{N}\tau$ -ligation that is conserved in all of the oxyTy and oxyHc structures.^[1a,b,2,23] $^{\text{S}}\text{P}_{4\text{MeImd}}$ represents the most structurally

faithful model to oxyTy, where 4-methylimidazole acts as a truncated histidine mimic that is expected to exhibit N π -ligation to the ^5P core based on its optical spectrum, while $^5\text{P}_{\text{HImd}}$ is the simplest imidazole-ligated ^5P species possible. The effect of $\text{Cu}^{\text{II}}_2\text{O}_2$ core exposure by minimizing imidazole steric demands and the importance of this work is realized in their reactivity towards H_2Asc at -145°C ; $^5\text{P}_{\text{1MeImd}}$ reacts stoichiometrically as an overall two H-atom acceptor, while $^5\text{P}_{\text{12Me2Imd}}$ only reacts in the presence of an excess of H_2Asc . This demonstrates that exposed $^5\text{P}_{\text{RImd}}$ cores facilitate substrate access to enhance reaction rates. Further evidence comes from the reaction of $^5\text{P}_{\text{1MeImd}}$ with phenolates to afford a transient phenolate-bonded bis- μ -oxide dicopper (III) $\text{Cu}^{\text{III}}_2\text{O}_2$ intermediate, the stabilization of which is enhanced by the lesser steric demands of N π -ligated imidazoles. The evolutionary selection of exclusive N π -ligated imidazole ligation in such dioxygen-activating copper enzymes may indeed be tied to accessing, albeit transiently, the higher Cu^{III} oxidation state, a non-intuitive functional advantage.

Acknowledgements

Use of the Stanford Synchrotron Radiation Lightsource, SLAC National Accelerator Laboratory, is supported by the U.S. Department of Energy, Office of Science, Office of Basic Energy Sciences under Contract No. DE-AC02-76SF00515. The SSRL Structural Molecular Biology Program is supported by the DOE Office of Biological and Environmental Research, and by the National Institutes of Health, National Institute of General Medical Sciences (including P41GM103393). The contents of this publication are solely the responsibility of the authors and do not necessarily represent the official views of NIGMS or NIH.

Keywords: coordination chemistry · copper dioxygen · extreme solution temperatures · N π imidazole ligation

How to cite: *Angew. Chem. Int. Ed.* **2016**, 55, 10453–10457
Angew. Chem. **2016**, 128, 10609–10613

- [1] a) Y. Matoba, T. Kumagai, A. Yamamoto, H. Yoshitsu, M. Sugiyama, *J. Biol. Chem.* **2006**, 281, 8981–8990; b) E. I. Solomon, D. E. Heppner, E. M. Johnston, J. W. Ginsbach, J. Cirera, M. Qayyum, M. T. Kieber-Emmons, C. H. Kjaergaard, R. G. Hadt, L. Tian, *Chem. Rev.* **2014**, 114, 3659–3853; c) S. Karlin, Z. Y. Zhu, K. D. Karlin, *Proc. Natl. Acad. Sci. USA* **1997**, 94, 14225–14230.
- [2] H. Decker, N. Hellmann, E. Jaenicke, B. Lieb, U. Meissner, J. Markl, *Integr. Comp. Biol.* **2007**, 47, 631–644.
- [3] a) T. Burmester, *J. Comp. Physiol. B* **2002**, 172, 95–107; b) T. Burmester, *Mol. Biol. Evol.* **2001**, 18, 184–195; c) T. Burmester, K. Scheller, *J. Mol. Evol.* **1996**, 42, 713–728.
- [4] a) M. Rolff, J. Schottenheim, H. Decker, F. Tuzek, *Chem. Soc. Rev.* **2011**, 40, 4077–4098; b) H. Claus, H. Decker, *Syst. Appl. Microbiol.* **2006**, 29, 3–14.
- [5] H. Decker, T. Schweikardt, F. Tuzek, *Angew. Chem. Int. Ed.* **2006**, 45, 4546–4550; *Angew. Chem.* **2006**, 118, 4658–4663.
- [6] C. Morioka, Y. Tachi, S. Suzuki, S. Itoh, *J. Am. Chem. Soc.* **2006**, 128, 6788–6789.
- [7] T. D. Wilson, Y. Yu, Y. Lu, *Coord. Chem. Rev.* **2013**, 257, 260–276.
- [8] a) N. Kitajima, T. Koda, S. Hashimoto, T. Kitagawa, Y. Moro-Oka, *J. Am. Chem. Soc.* **1991**, 113, 5664–5671; b) W. E. Lynch, D. M. Kurtz, S. K. Wang, R. A. Scott, *J. Am. Chem. Soc.* **1994**, 116, 11030–11038; c) T. N. Sorrell, W. E. Allen, P. S. White, *Inorg. Chem.* **1995**, 34, 952–960; d) M. Kodera, K. Katayama, Y. Tachi, K. Kano, S. Hirota, S. Fujinami, M. Suzuki, *J. Am. Chem. Soc.* **1999**, 121, 11006–11007; e) N. Kitajima, Y. Moro-Oka, *Chem. Rev.* **1994**, 94, 737–757; f) L. M. Mirica, X. Ottenwaelde, T. D. P. Stack, *Chem. Rev.* **2004**, 104, 1013–1045; g) E. A. Lewis, W. B. Tolman, *Chem. Rev.* **2004**, 104, 1047–1076; h) L. Q. Hatcher, K. D. Karlin, in *Advances in Inorganic Chemistry Including Bioinorganic Studies*, Vol. 58, Elsevier, Amsterdam, **2006**, pp. 131–184.
- [9] a) A. Hoffmann, C. Citek, S. Binder, A. Goos, M. Rübhausen, O. Troeppner, I. Ivanović-Burmazović, E. C. Wasinger, T. D. P. Stack, S. Herres-Pawlis, *Angew. Chem. Int. Ed.* **2013**, 52, 5398–5401; *Angew. Chem.* **2013**, 125, 5508–5512; b) K. V. N. Esguerra, Y. Fall, L. Petitjean, J.-P. Lumb, *J. Am. Chem. Soc.* **2014**, 136, 7662–7668; c) J. Schottenheim, C. Gernert, B. Herzigkeit, J. Krahmer, F. Tuzek, *Eur. J. Inorg. Chem.* **2015**, 3501–3511.
- [10] C. Citek, C. T. Lyons, E. C. Wasinger, T. D. P. Stack, *Nat. Chem.* **2012**, 4, 317–322.
- [11] Y. Lee, G. Y. Park, H. R. Lucas, P. L. Vajda, K. Kamaraj, M. A. Vance, A. E. Milligan, J. S. Woertink, M. A. Siegler, A. A. Narducci Sarjeant, L. N. Zakharov, A. L. Rheingold, E. I. Solomon, K. D. Karlin, *Inorg. Chem.* **2009**, 48, 11297–11309.
- [12] A. D. Zuberbühler, in *Copper Coordination Chemistry, Biochemical and Inorganic Perspectives* (Eds.: K. D. Karlin, J. Zubietta), Adenine Press, Guilderland, NY, **1983**, pp. 237–258.
- [13] a) I. Sanyal, R. W. Strange, N. J. Blackburn, K. D. Karlin, *J. Am. Chem. Soc.* **1991**, 113, 4692–4693; b) I. Sanyal, K. D. Karlin, R. W. Strange, N. J. Blackburn, *J. Am. Chem. Soc.* **1993**, 115, 11259–11270; c) A. D. Zuberbühler, in *Bioinorganic Chemistry of Copper* (Eds.: K. D. Karlin, Z. Tyeklár), Chapman & Hall, New York, **1993**, pp. 264–276.
- [14] a) C. Citek, J. B. Gary, E. C. Wasinger, T. D. P. Stack, *J. Am. Chem. Soc.* **2015**, 137, 6991–6994; b) C. Citek, S. Herres-Pawlis, T. D. P. Stack, *Acc. Chem. Res.* **2015**, 48, 2424–2433; c) C. Citek, B.-L. Lin, T. E. Phelps, E. C. Wasinger, T. D. P. Stack, *J. Am. Chem. Soc.* **2014**, 136, 14405–14408.
- [15] V. Mahadevan, J. L. DuBois, B. Hedman, K. O. Hodgson, T. D. P. Stack, *J. Am. Chem. Soc.* **1999**, 121, 5583–5584.
- [16] a) L. S. Kau, D. J. Spira-Solomon, J. E. Penner-Hahn, K. O. Hodgson, E. I. Solomon, *J. Am. Chem. Soc.* **1987**, 109, 6433–6442; b) J. L. DuBois, P. Mukherjee, A. M. Collier, J. M. Mayer, E. I. Solomon, B. Hedman, T. D. P. Stack, K. O. Hodgson, *J. Am. Chem. Soc.* **1997**, 119, 8578–8579.
- [17] G. Y. Park, M. F. Qayyum, J. Woertink, K. O. Hodgson, B. Hedman, A. A. N. Sarjeant, E. I. Solomon, K. D. Karlin, *J. Am. Chem. Soc.* **2012**, 134, 8513–8524.
- [18] a) P. K. Ross, E. I. Solomon, *J. Am. Chem. Soc.* **1991**, 113, 3246–3259; b) E. I. Solomon, P. Chen, M. Metz, S. K. Lee, A. E. Palmer, *Angew. Chem. Int. Ed.* **2001**, 40, 4570–4590; *Angew. Chem.* **2001**, 113, 4702–4724.
- [19] R. L. Martin, *J. Chem. Phys.* **2003**, 118, 4775–4777.
- [20] J. J. Warren, T. A. Tronic, J. M. Mayer, *Chem. Rev.* **2010**, 110, 6961–7001.
- [21] Phenolate binding to a diamine-ligated SP species have been previously observed to yield a transient phenolate-bonded bis- μ -oxide dicopper (III) intermediate, which exhibits similar optical features to the intermediate from this work.
- [22] a) S. Itoh, S. Fukuzumi, *Acc. Chem. Res.* **2007**, 40, 592–600; b) J. L. Muñoz-Muñoz, J. Bernal, M. d. M. García-Molina, F. García-Molina, P. A. García-Ruiz, R. Varon, J. N. Rodríguez-Lopez, F. García-Canovas, *Biochem. Biophys. Res. Commun.* **2012**, 424, 228–233; c) L. M. Mirica, M. Vance, D. J. Rudd, B. Hedman, K. O. Hodgson, E. I. Solomon, T. D. P. Stack, *Science*

2005, 308, 1890–1892; d) E. Solem, F. Tuzek, H. Decker, *Angew. Chem. Int. Ed.* **2016**, 55, 2884–2888; *Angew. Chem.* **2016**, 128, 2934–2938.

[23] C. J. Rolle, C. Saracini, K. D. Karlin, in *Encyclopedia of Inorganic and Bioinorganic Chemistry*, Wiley, Hoboken, **2011**.

Received: May 26, 2016

Revised: June 30, 2016

Published online: July 21, 2016
